ELSEVIER

Spectrochimica Acta Part B 61 (2006) 545 – 553

SPECTROCHIMICA ACTA PART B

www.elsevier.com/locate/sab

Nanometric resolution in glow discharge optical emission spectroscopy and Rutherford backscattering spectrometry depth profiling of metal (Cr, Al) nitride multilayers

R. Escobar Galindo [a,*], R. Gago [b], E. Forniés [a], A. Muñoz-Martín [c], A. Climent Font [b], J.M. Albella [a]

[a] *Instituto de Ciencia de Materiales de Madrid, Consejo Superior de Investigaciones Científicas, E-28049 Madrid, Spain*
[b] *Centro de Micro-Análisis de Materiales and Departamento de Física Aplicada, Universidad Autónoma de Madrid, E-28049 Madrid, Spain*
[c] *Centro de Micro-Análisis de Materiales y Parque Científico de Madrid, Campus de Cantoblanco, E-28049 Madrid, Spain*

Received 27 January 2006; accepted 29 March 2006
Available online 19 May 2006

Abstract

In this work, we address the capability of glow discharge optical emission spectroscopy (GDOES) for fast and accurate depth profiling of multilayer nitride coatings down to the nanometer range. This is shown by resolving the particular case of CrN/AlN structures with individual thickness ranging from hundreds to few nanometers. In order to discriminate and identify artefacts in the GDOES depth profile due to the sputtering process, the layered structures were verified by Rutherford backscattering spectrometry (RBS) and scanning electron microscopy (SEM). The interfaces in the GDOES profiles for CrN/AlN structures are sharper than the ones measured for similar metal multilayers due to the lower sputtering rate of the nitrides. However, as a consequence of the crater shape, there is a linear degradation of the depth resolution with depth (approximately 40 nm/μm), saturating at a value of approximately half the thickness of the thinner layer. This limit is imposed by the simultaneous sputtering of consecutive layers. The ultimate GDOES depth resolution at the near surface region was estimated to be of 4–6 nm.
© 2006 Elsevier B.V. All rights reserved.

Keywords: GDOES analysis; RBS analysis; Multilayer; Depth resolution

1. Introduction

In the last decades, metal and/or metal compound coatings are being used extensively in a wide range of applications, either as hard protective coatings for mechanical parts and tools or as optical coatings for lenses and architecture glass panels. Other applications include their use as barrier contacts for microelectronics, or in biomedical prosthesis. Generally, most of these requirements cannot be accomplished with only one material compound and nowadays there is intensive research on multilayer and composite coatings, where the properties of different coating materials are combined and optimised to obtain the desired properties. Of special relevance is the case of hard multilayer coatings with bilayer period in the order of some nanometers (superlattices), which are designed to reach film hardness in the range of superhard materials (>40 GPa) [1–5]. In these and other applications, sharp interfaces and a low degree of mixing between the component materials are strictly required. The addition of an adhesive interlayer (generally, Cr or Ti) and/or a top functional layer is also a common practice to tailor the desired surface properties, e.g. low friction, optical reflectivity, corrosion resistance, etc.

Obviously, the attainment of these complex structures needs high resolution analytical techniques to get information about surface and depth composition at nanometric level. Rutherford backscattering spectrometry (RBS) is a non-destructive technique that is commonly employed for in-depth compositional analysis of metal and metal nitride layers. The technique presents a high elemental sensitivity for heavy

* Corresponding author. Tel.: +34 91 3721420x304.
E-mail address: rescobar@icmm.csic.es (R. Escobar Galindo).

0584-8547/$ - see front matter © 2006 Elsevier B.V. All rights reserved.
doi:10.1016/j.sab.2006.03.012

elements (<1 at.%), a depth resolution in the nanometer range (∼5–10 nm) and it does not require standards for quantification. The main drawbacks of RBS are, besides the requirement of large-scale instrumentation (electrostatic accelerators or another ion source), the limitation of the analysis to the very first microns of the sample, the difficult analysis of light elements on substrates with higher mass number and the considerable resolution decrease at increasing depths due to energy straggling of the incoming beam. In order to keep nanometer resolution at larger depths, surface spectroscopies, such as X-ray photoelectron spectroscopy (XPS) or Auger electron spectroscopy (AES) are generally used for this purpose. However, these methods suffer from preferential sputtering, because the surface itself is analysed, and not the sputtered material. Secondary ion mass spectroscopy (SIMS) equipped with sputtering depth profiling (destructive methods) is a suitable alternative though, in routine process development, rapid analysis is required to provide feedback information on the effect of the deposition conditions. Glow discharge optical emission spectroscopy (GDOES) is a well-established technique capable to meet such demands. The method is based on the detection of the emitted light of the excited atoms sputtered from the sample surface by a glow discharge. Only moderate vacuum is required, and the sputtering and sampling rates are high enough to obtain a compositional profile of some microns depth in a few minutes, with a depth resolution in the nanometer range [6–11]. Besides, the use of a radio frequency (rf) source for sputtering extends the application of GDOES to the study of insulators both as coatings and as substrates [12,13].

In previous papers [14,15], we have analyzed multilayer stacks of pure metals (Ti/Cr) by GDOES and have studied the artefacts affecting depth resolution, demonstrating its capability to analyze layers down to the nanometer range, even in layers buried at depths larger than 1 µm. As in the case of etching-based depth profiling techniques, the major issues degrading the depth profiles and resolution in GDOES are related with ion beam mixing of layers and the contributions arising from the special crater shape [16–18]. The capability to resolve and delimit such GDOES artefacts in the analysis of metal oxides and nitride superlattices structures is relevant from the point of view of their wide range of applications. Therefore, the extensively used CrN/AlN multilayer coatings have been selected in this work to be analysed by GDOES. The results have been contrasted with RBS to assess the as-deposited multilayer structure (composition, periodicity, interface quality and degree of layer mixing). In order to determine the resolution limits of the GDOES technique and the influence of the materials sequence, nitride multilayers stacks with decreasing bilayer thickness as well as ultra-thin nitride layers buried at increasing depths in a thicker matrix have been analysed. Previous GDOES-RBS results on nitride system *n*(TiN/AlN) has been reported by Thobor et al. [19], though this work deals only with very few (*n* = 1, 2) thick layers showing rough interfaces. Although there has been an extensive work done regarding the GDOES depth resolution in multilayers (mostly in metal systems) [20–28], to our knowledge, no systematic work on the assessment of the depth resolution in both GDOES and RBS techniques on metal nitride multilayer systems has been done to date.

2. Experimental

2.1. CrN/AlN multilayer coating deposition

CrN/AlN multilayer coatings with individual thickness in the range of 5–500 nm and different material sequence were deposited to study the effect of the layer thickness and the interface nature on the depth profiles by GDOES and, additionally, to explore the resolution limits of the technique. The deposition of the multilayers was performed in a conventional planar DC magnetron sputtering system using two sputtering sources, placed 6.5 cm away from the substrate holder. The holder can be rotated to face the sample to each sputtering source and is provided with automatic position controller in order to control the deposition time for each layer. The deposition rates of the specimens were 135 Å min^{-1} for chromium nitride and 50 Å min^{-1} for aluminium nitride. Details of the sputtering system have been described elsewhere [29]. The base pressure was approximately 2×10^{-4} Pa and the working pressure was in the range 0.16–0.23 Pa. The cathode power was held constant at 100 W. No bias voltage was applied to the substrate holder by a DC power supply. Prior to deposition, 20 min of pre-sputtering was performed in order to remove the metal-nitride layer of the cathodes due to previous deposits. The metal targets used were commercial plates of very high purity. A mixture of Ar (99.999%) an N_2 (99.9992%) gases was introduced in the vacuum chamber. The N_2 relative flow rate (fr_{N_2}) was fixed to be 70% of the total flow rate (f_{tot} = 11 sccm) by changing simultaneously both Ar and N_2 flow rates.

The multilayer nitride coatings were deposited with a 100-nm Cr interlayer to improve adherence to the substrate. The coatings were all deposited onto Si(100) substrates. Table 1 gives a summary of the coatings studied in this work.

2.2. Multilayer characterization

The shape and depth of the sputtering crater and the coating thickness were measured by profilometry utilizing a Dektak 3030 surface profilometer. Scanning Electron Microscopy (SEM) micrographs of the multilayer structure were obtained

Table 1
Description of the studied coating systems. All coatings were deposited onto (100) silicon

Sample	Coating structure
Thick trilayer	380 nm CrN/470 nm AlN/380 nm CrN
	410 nm AlN/410 nm CrN/410 nm AlN
Thin multilayer	10× (35 nm CrN/100 nm AlN) + 100 nm Cr
	10× (50 nm AlN/70 nm CrN) + 100 nm Cr
Ultrathin multilayer	50× (10 nm AlN/10 nm CrN) + 100 nm Cr
	8x (10 nm AlN/10 nm CrN) + 100 nm Cr
Delta Markers AlN	10× (5 nm AlN/200 nm CrN) + 100 nm Cr

by a HITACHI S-2700 model using an accelerating potential of 15 kV.

RBS experiments were performed with the 5 MV HVEE Tandetron at the Centro de Micro-Análisis de Materiales [30] of Universidad Autónoma de Madrid. The RBS analysis is used, in combination with SEM, to confirm the layered structure of the coatings and to account for the quality of the multilayer interfaces. The RBS spectra were collected with He ions at an ion dose of 10 μC and ion energies of 1.5, 2 and 3.5 MeV. The analysis at different ion energies provides complementary information about the coating structure, i.e. higher surface sensitivity at 1.5 MeV whereas higher penetration depth together with non-Rutherford cross-section ($\sigma \sim 2\sigma_R$) [31] for the $^{14}N(\alpha, \alpha)^{14}N$ process is achieved at 3.5 MeV. The data were acquired simultaneously with two silicon surface barrier detectors located at scattering angles of 170° and 165°, respectively, and with an energy resolution of 15 keV. The experimental spectra were fitted with the program SIMNRA [32].

GDOES depth profile analysis of the coatings was completed using a Jobin Yvon RF GD Profiler [33] equipped with a 4-mm-diameter anode and operating at a typical radio frequency discharge pressure of 650 Pa and power of 40 W. The chamber was cleaned by sputtering a silicon (100) sample for 20 min. Before every experiment the samples were flushed with argon during 60 s. The sputtering rates of the studied elements were measured to be of 4.2, 3.4 and 2.5 μm min^{-1} for chromium nitride, silicon and aluminium nitride, respectively. The high etching rates obtained during GDOES analysis resulted in very short experimental times (below 1 min of operation). A collection rate of 200 points/s was used to measure all the samples. Quantified profiles were obtained automatically using the standard Jobin Yvon QUANTUM Intelligent Quantification (IQ) software. The setup was calibrated using standard materials of known composition. In order to improve the quantification of nitrogen, we have used a series of chromium nitride coatings deposited by magnetron sputtering in our laboratory. The composition of these homemade standards was assessed by RBS.

3. Results and discussion

3.1. Characterization of the metal nitride multilayers: RBS and SEM results

The deposited metal nitride multilayers were, in a first stage, characterised by SEM and RBS techniques in order to confirm the layered structure and obtain information about the quality of the interfaces. As illustrative examples, Fig. 1(a) and (b) show cross sectional SEM micrographs of CrN/AlN layered structures with thick and thin layers, respectively. Fig. 1(a) corresponds to a CrN/AlN/CrN trilayer on Si(100) with a total thickness of 1.2 μm and individual layers of 380, 470 and 380 nm, respectively, as measured by SEM and profilometry. The coating presents a pronounced columnar morphology probably due to the absence of bias voltage during the sputtering deposition [34]. It has been argued in the literature

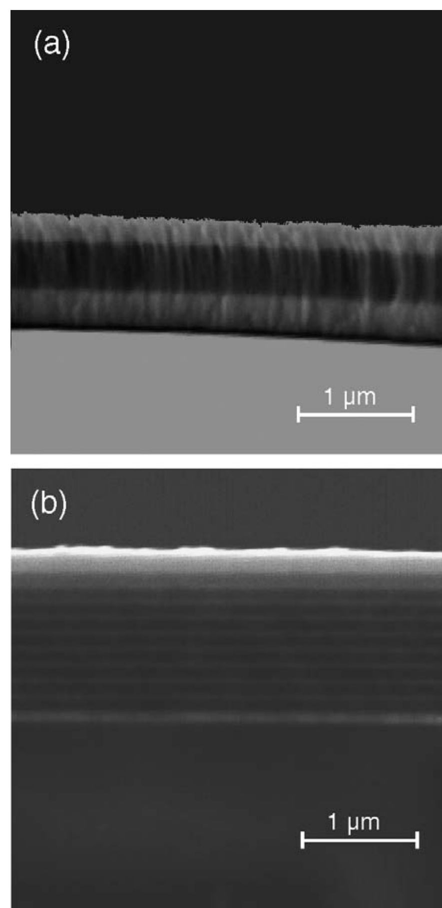

Fig. 1. SEM micrographs of (a) trilayer 380 nm CrN/470 nm AlN/380 nm CrN and (b) multilayer 10× (35 nm CrN/100 nm AlN)/100 nm Cr.

[19] that the columnar structure observed in the case of (TiN/AlN) multilayer coatings induce smooth interfaces. However, as will be shown later, in our deposited films RBS data yields well defined interfaces up to the limit of the technique (5–10 nm). Fig. 1(b) shows a CrN/AlN multilayer coating with a total thickness of 1.45 μm, where alternating CrN and AlN layers of 35 and 100 nm, respectively, are clearly observed. The coating has 10 bilayer periods and a 100 nm Cr interlayer to improve the adhesion to the Si(100) substrate.

Fig. 2 shows illustrative RBS spectra for CrN/AlN layered structures composing individual layers of hundreds on nanometers (panel a) and tens of nanometers (panels b and c). The experimental data and the global fit results have been shifted vertically from the contributions of the elemental spectra (lower part of the graphs) for clarity purposes. The definition of the layered structure is quite evident by the oscillations in the experimental data. The samples were also measured at lower ion energies to increase the depth resolution (at the near surface), yielding the same fitting results as in the high-energy spectra.

The capability of RBS to resolve layers with a few nanometer thickness without the use of high-resolution detectors (for example, magnetic spectrographs) is not direct, since the success depends on the specific sample and the experimental configuration. In the case of CrN/AlN layers of a few nanometers, Fig. 3 shows that the layered structure can be

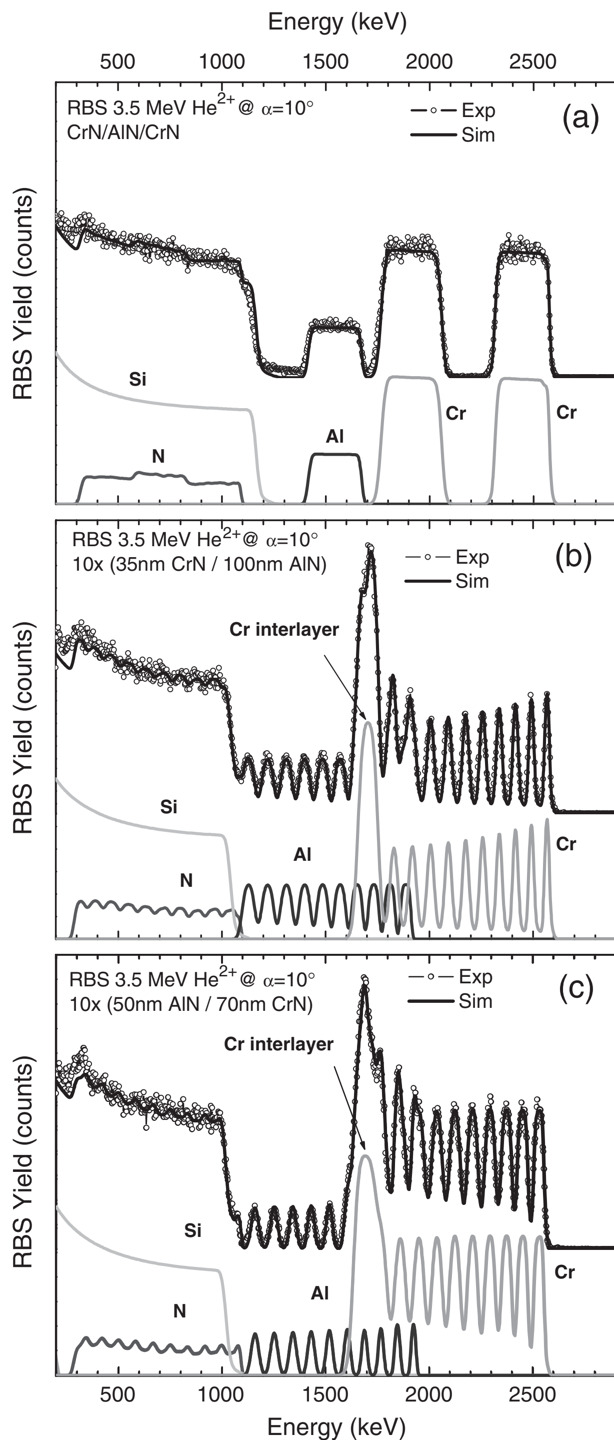

Fig. 2. RBS profiles of (a) trilayer 380 nm CrN/470 nm AlN/380 nm CrN; (b) multilayer 10× (35 nm CrN/100 nm AlN)/100 nm Cr and (c) multilayer 10× (50 nm AlN/70 nm CrN)/100 nm Cr. All the experiments were performed using an ion energy of 3.5 MeV and under an incidence angle of 10°. The experimental data and the global fit results have been shifted vertically from the contributions of the elemental spectra (lower part of the graphs).

resolved by standard RBS when using ion energies ≤2 MeV, thus increasing the depth resolution. In the case of both CrN and AlN layers in the few nanometer range (Fig. 3a), the samples were measured at large incidence angle (45°) to increase the effective layer thickness. However, Fig. 3(b) shows that AlN layers of 5 nm embedded in a heavier matrix, such as in the case of CrN, are easily resolved under normal incidence. These AlN "markers" are alternating with 200 nm CrN layers (the sample starts with a 5-nm AlN layer at the surface). The total coating thickness was 2.1 μm as measured by profilometry.

In all the cases, the RBS fitting assumes a coating structure with sharp interfaces. The agreement between the experimental and fitted spectra is quite good, which confirms the well-defined layered structure of the coatings. The RBS analysis also corroborates that the metal nitride layers stoichiometry (Me/N) in the coatings is almost 1:1. However, a small oxygen contamination (3–5 at.%) had to be included in the simulation for the CrN layers, mostly at large depths. The presence of O cannot be directly observed in the spectra due to its relatively low content and the presence of heavier elements in the sample matrix. However, it can be indirectly extracted from the deficient content of metal elements and N, where the signal

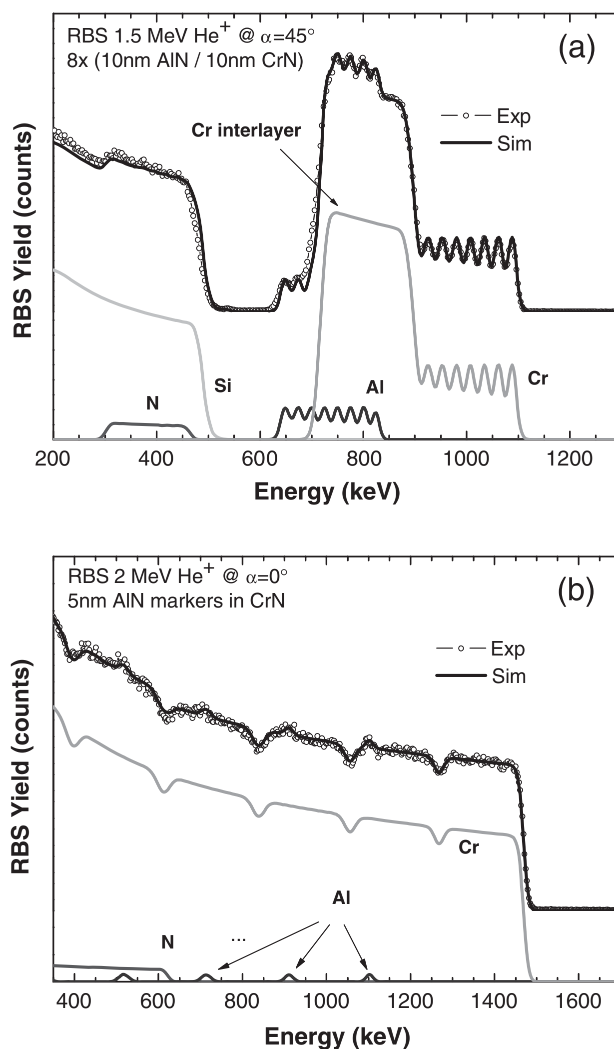

Fig. 3. RBS profiles of (a) multilayer 50× (10 nm AlN/10 nm CrN)/100 nm Cr using a ion energy of 1.5 MeV and under and incidence angle of 45° and (b) multilayer 10× (5 nm AlN/200 nm CrN)/100 nm Cr using an ion energy of 2.0 MeV and under an incidence angle of 0°. The experimental data and the global fit results have been shifted vertically from the contributions of the elemental spectra (lower part of the graphs).

Table 2
Fitting results from the RBS analysis. The errors are derived from the fitting procedure. The corresponding thickness for 10^{15} at/cm^2 of CrN, AlN and Cr is 0.10, 0.11 and 0.12 (± 0.02) nm, respectively.

SEM/Profilometry (nm)	RBS (1015 at/cm$_2$)
380 CrN/470 AlN/380 CrN	3550±50 CrN/4350±50 AlN/3600±50 CrN
10× (35 CrN/100 AlN)/100 Cr	10× (360±20 CrN/930±30 AlN)/780±50 Cr
10× (50 AlN/70 CrN)/100 Cr	10× (470±30 AlN/720±20 CrN)/850±50 Cr
8× (10 AlN/10 CrN)/100 Cr	8× (80±30 AlN/70±20 CrN)/740±50 Cr
10× (5 AlN/200 CrN)/100 Cr	10× (40±10 AlN/2050±20 CrN)

can be clearly fitted (note that at 3.5 MeV the scattering cross-section for N is $\sigma \sim 2\sigma_{\mathrm{Rutherford}}$). The analysis also indicates a good control over the layer thickness during the growth process of alternate materials, since the thickness of the individual CrN and AlN layers in the multilayer structure is quite reproducible. No effect of the materials sequence in the RBS profiles of the nitride multilayers was observed, as shown by the comparison of panels (b) and (c) of Fig. 2.

Table 2 summarises the fitting results of the samples analysed by RBS. As stated before, the layered structure of the samples is well defined with an interface width of 5–10 nm (given by the resolution limit of the technique at the near surface region). The depth resolution by RBS deteriorates at increasing analysis depths due to ion beam straggling, although this effect is included in the simulation code. The effect of energy straggling is clearly appreciated in Fig. 2(b) and (c) by the increase in the width of the Cr and Al signals at larger depths (lower energy). It should be also pointed out that the scattering cross-section depends as $\sigma \sim 1/E_{\mathrm{ion}}^2$ and, therefore, the relative yield corresponding to layers from the same nitride material should increase at larger depths (lower energies). In this sense, the progressive decrease in height of the Cr signal shown in Fig. 2(b) is, therefore, a clear indication of the oxidation of the inner layers, as stated before. Finally, in the case of multilayer structures, the top-most CrN layers are better resolved since they appear without any background in the high-energy side of the spectra whereas the AlN layers overlap with the signal from inner CrN layers.

3.2. GDOES depth profiling of the nitride multilayers

Once the nitride multilayer systems were properly characterized, we analysed them by GDOES. The depth resolution of the technique will be further discussed in Section 3.3. As stated by RBS, both the multilayer period and composition are very homogeneous through all the coating and the interfaces. Hence, variations observed in the GDOES profiles must be attributed to specific artefacts of the technique. Fig. 4 shows the GDOES profiles of CrN/AlN multilayer structures with layer thickness ranging from 500 to 10 nm.

The profile for the CrN/AlN/CrN trilayer (see Table 1 for thickness values) is displayed in Fig. 4(a), showing an excellent agreement on the individual layer thickness, as well as on the coating stoichiometric composition. Nevertheless, typical GDOES features can be observed. Prior to each interface, there is a rise of the major component of the subsequent layer (Al, Cr and Si, respectively) due to the non-flat geometry of the crater, i.e., the presence of a well at the edge of the crater. This well is mainly due to the geometry of the Grimm source cell [18] and, although it can be minimized by changing the discharge parameters (mainly pressure and power), it cannot be fully eliminated. After the interfaces, there is also an increasing tail of the precedent major element (Cr, Al and Cr and N, respectively) that in a previous work [14] we have ascribed to

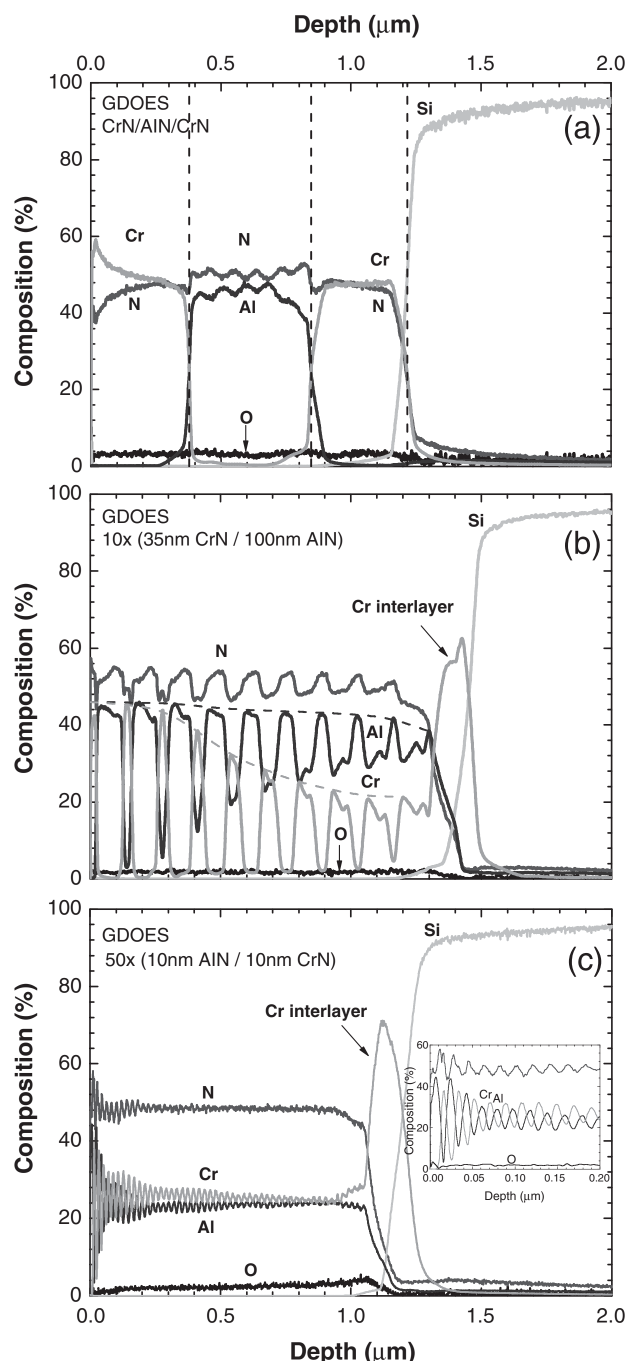

Fig. 4. GDOES depth profiles of (a) trilayer 380 nm CrN/470 nm AlN/ 380 nm CrN; (b) multilayer 10× (35 nm CrN/100 nm AlN)/100 nm Cr and (c) 50× (10 nm AlN/10 nm CrN)/100 nm Cr. The dashed vertical lines in (a) indicate the location of the different interfaces. The dashed lines in (b) show the decrease of the metal content. The inset in (c) represents the first 200 nm of the depth profile.

the sputtering of redeposited material on the crater walls, e.g. due to a conical shape of the crater. Regardless these artefacts, the interfaces between the nitride layers are very sharp as shown in Section 3.3.

Additional GDOES effects in the profiles of Fig. 4(a), include the wavy profile observed for the insulating AlN layer. This behaviour cannot be attributed to surface charging, as such effect is practically insignificant in GDOES experiments [26]. Instead, we attribute the periodic modulation to optical interferences of the transparent AlN film [35,36]. Thus, the five oscillations, with a period of 90 nm, observed in the Al profiles (although the last Al peak is hindered by the crater edge effect) nicely match the Bragg equation for normal incidence ($\cos\theta = 1$),

$$N\lambda = 2nd$$

where N is an integral for constructive interference, λ is the wavelength of the emitted photons (396 nm for aluminium), n de refraction index (2.11 for AlN [37]) and d the thickness of the layer (470 nm in this case). In fact, we have also observed the same behaviour in a single 600 nm AlN layer on silicon, where six oscillations with the same period of 90 nm were detected in the Al profile. The oscillations observed in the N profile are due to the quantification procedure. The N signal at 149 nm show no oscillations in the qualitative profile most probably because most layers are not transparent below 200 nm and N should have about twice of the oscillations [36].

It is also remarkable that, although it is difficult to asses strong conclusions regarding oxygen due to the lack of calibration samples, there is a very good agreement on the oxygen content in the coating measured by both techniques. The 4% oxygen detected by GDOES is present within the overall coating profile, probably due to the inter-diffusion caused by the GDOES sputtering, while in RBS was only present in the CrN layers.

Fig. 4(b) shows the depth profile for the multilayer system with alternating 35 nm CrN and 100 nm AlN layers. The GDOES depth profile properly reproduces the multilayer structure of the coating. The ten nitride bilayers are perfectly identified, although severe signal degradation with depth is observed. Until a depth of approximately 500 nm, the thicker AlN layers show a very square profile and the interfaces with the thinner CrN layers are very sharp, showing very low layer mixing. The maximum Al content decreases less than a 7% for the first eight bilayers and only before the interface with the adhesive Cr layer it lowers down to a 17% of the original value (see Fig. 5a). On the other hand, the Cr intensity of the thinner CrN layers rapidly decreases more than 35% in the first six layers and, from this depth on, the major metallic element detected in the CrN layers is no longer chromium but aluminium. This result is similar to the one observed for metallic multilayers [15]. The main difference deals with the GDOES-measured thickness of the individual layers. In metallic Cr/Ti multilayers, both the individual chromium and titanium layers were broadening progressively with depth. On the contrary, in the nitride multilayer studied in this work, a different behaviour is observed as shown in Fig. 5(b). Within the first sputtered 500 nm, the measured thickness of both the CrN (32–38 nm) and the AlN (101–93 nm) layers

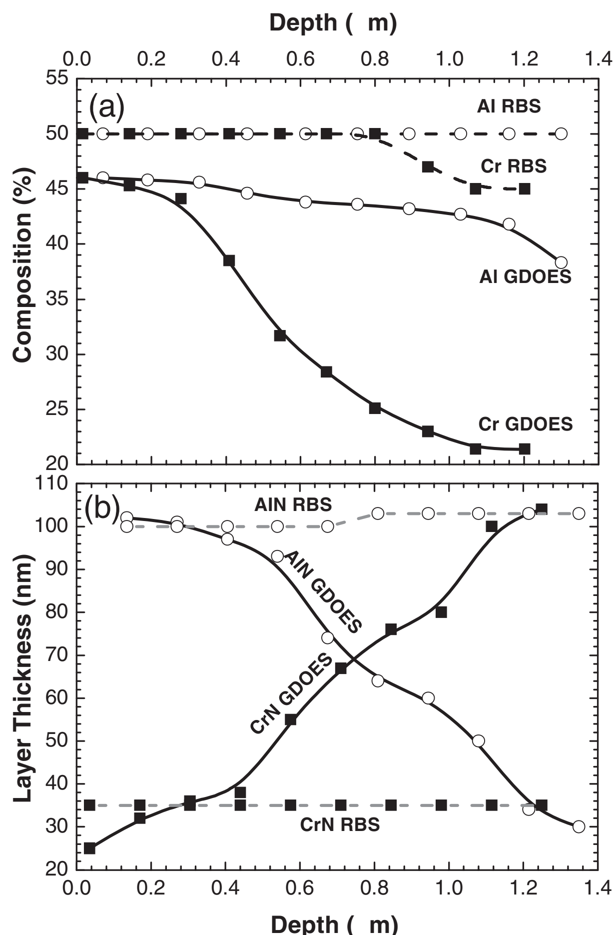

Fig. 5. RBS and GDOES comparison of (a) metal composition and (b) layer thickness versus depth in the case of the multilayer 10× (35 nm CrN/100 nm AlN.

corresponds nicely to the expected, and confirmed by RBS, nominal thicknesses. After then, there is a monotonous increase (decrease) of the thickness of the CrN (AlN) layers, until the last two bilayers, where a complete inversion of the thickness values occurs. The initially thinner CrN layer (35 nm) is measured to be of more than 100 nm, while the thicker AlN (100 nm) is at the last layers measured to be of only 30 nm. Nevertheless, the bilayer period $\Lambda = 135$ nm is conserved within the coating. These profiles reveal that several layers are being sputtered at the same time due to the crater roughening and the change in the crater shape during GDOES experiment.

Regarding the ultrathin coatings of 50 bilayers of alternating 10 nm AlN and 10 nm CrN, it can be observed in Fig. 4(c) that GDOES is able to resolve all the 100 layers. Although there is a high mixing of the layers, all the Cr and Al peaks are perfectly identified and the bilayer period of 20 nm maintained within the overall coating (see inset in Fig. 4c). This is a very good result for an experiment that takes only 25ss to analyze the whole multilayer. RBS measurements are also rapid in comparison with other surface analysis techniques (i.e. SIMS), though they are constrained by both the access to beam-time and the evacuation time for ultra-high vacuum (typically several hours).

3.3. GDOES depth resolution analysis of the nitride multilayers

The depth resolution (interface width) is commonly defined as the measured depth over which the signal of an element varies from 84% to 16% [38,39]. However, the prerequisite for using such definition is that the profile can be approximated as an error function, which is not valid in general for GDOES profiles due to the crater shape artefacts described above [18,40]. Therefore, the use of the "inverse maximum slope" method has been suggested [41]. In this method, the depth resolution is defined as the ratio between the difference of the corresponding element concentration between two layers (Δc) and the steepest slope of the quantified depth profile at their interface, defined as $(dc/dz)_{max}$:

$$\Delta z = \frac{\Delta c}{(dc/dz)_{max}}$$

In Fig. 6, the derivative of the GDOES profile of Fig. 4(a) is plotted versus the sputtered depth, to show how to obtain the depth resolution. By doing so, the first CrN/AlN interface, located at 380 nm, was measured to be of 19 ± 4 nm, increasing up to 33 ± 5 nm for the subsequent AlN/CrN interface at 850 nm. As described in [42], such interface widths are considerably lower that the ones previously obtained, for metal Cr/Ti trilayers [14] probably due to a lower sputtering rate of the nitrides. It is important to note that this comparison must be done for similar interface depths.

In the reversed AlN/CrN/AlN/Si system (each layer with at thickness of 410 nm), slight differences were found for the interface widths measured by GDOES: 22 ± 3 and 39 ± 9 nm for AlN/CrN (at 405 nm) and CrN/AlN (at 815 nm) interfaces, respectively. Therefore, we could estimate that the depth resolution of the CrN/AlN interfaces worsens some 40 nm for each micron where the interface is placed in, while the AlN/CrN interface degrades 50 nm/μm with an initial depth resolution at the surface of about 6 nm (see Fig. 7). As mentioned before, the loss of resolution with depth during GDOES experiments is

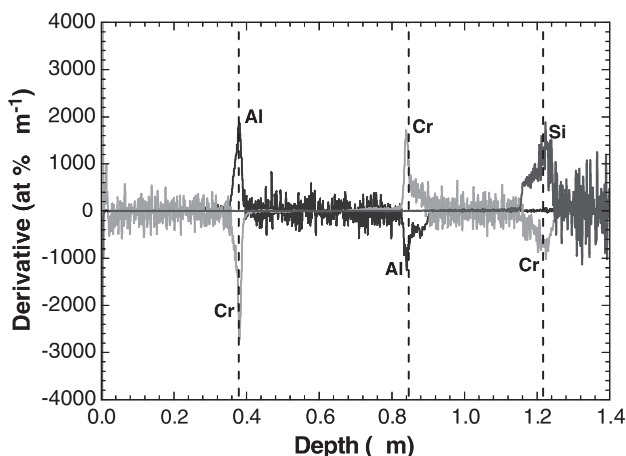

Fig. 6. Derivative of the depth profile of Fig. 4(a) is plotted versus depth to obtain the depth resolution following "maximum inverse slope" method. The dashed vertical lines indicate the location of the different interfaces.

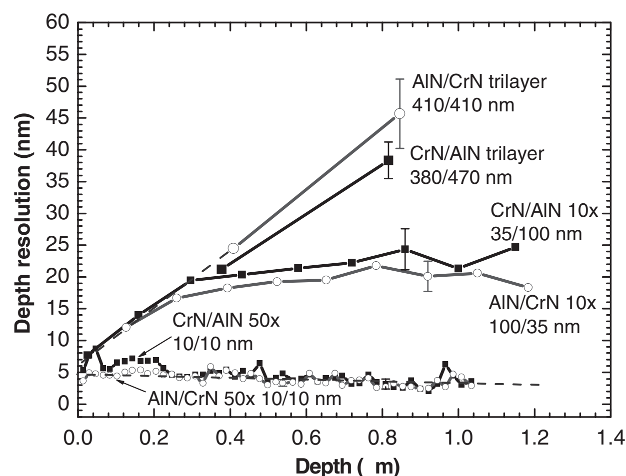

Fig. 7. Variation of the depth resolution with the sputtering depth for the different interfaces studied by GDOES. Open circles are used to represent the depth resolution of AlN/CrN interfaces and closed squares for CrN/AlN interfaces. The dashed lines show the extrapolation of the results to the surface.

much lower in nitride multilayers than in the pure metals (i.e. 154 ± 46 nm μm^{-1} for Ti/Cr interfaces). Associated to this, the different interfacial results changing the order of the materials present at the interface ($A/B \neq B/A$), obtained in metal multilayers, are also observed for nitrides, although the differences are much smaller. This difference cannot be explained in terms of differences in interface roughness, as done by Thobor et al. [19] for (TiN/AlN) multilayers. In our case, both interfaces are very sharp as stated by RBS measurements, so the different interface widths measured has to do with the particular shape of the crater before and after each interface as well as with the differences in the relative sputtering rates.

As in the case of thicker coatings, we have used the profile derivatives of Cr, Al and Si, to estimate the degradation of resolution depth at increasing etched depth for the multilayer system with alternating 35 nm CrN and 100 nm AlN layers (see Fig. 7). Initially, there is a similar linear increase of the depth resolution of about 40 nm/μm for both CrN/AlN and AlN/CrN interfaces. Making an extrapolation of this dependence to the origin leads to a depth resolution of less than 7 nm at the surface. This behaviour is observed until a depth of approximately 400 nm, corresponding quite nicely with the range where the thickness of the layers is properly determined (see Fig. 5b). Beyond this depth and related to the mixing of the consecutive layers, there is decrease in the slope of the depth resolution and a final saturation around a value of 20 nm. In principle, it may appear contradictory the fact that the depth resolution saturates when the profiles are clearly worsening. However, as Angeli et al. have accurately pointed out [18], the physical meaning of the depth resolution is the crater volume which sputters a certain type of layer (material). Therefore, if the crater sputters several bilayers at the same time, all of them contribute to improve the depth resolution value.

The depth resolution of the ultrathin coatings of 50 bilayers of alternating 10 nm AlN and 10 nm CrN was again derived using the derivative of the profiles of Fig. 4(c). It can be observed in Fig. 7 how the depth resolution of the first three

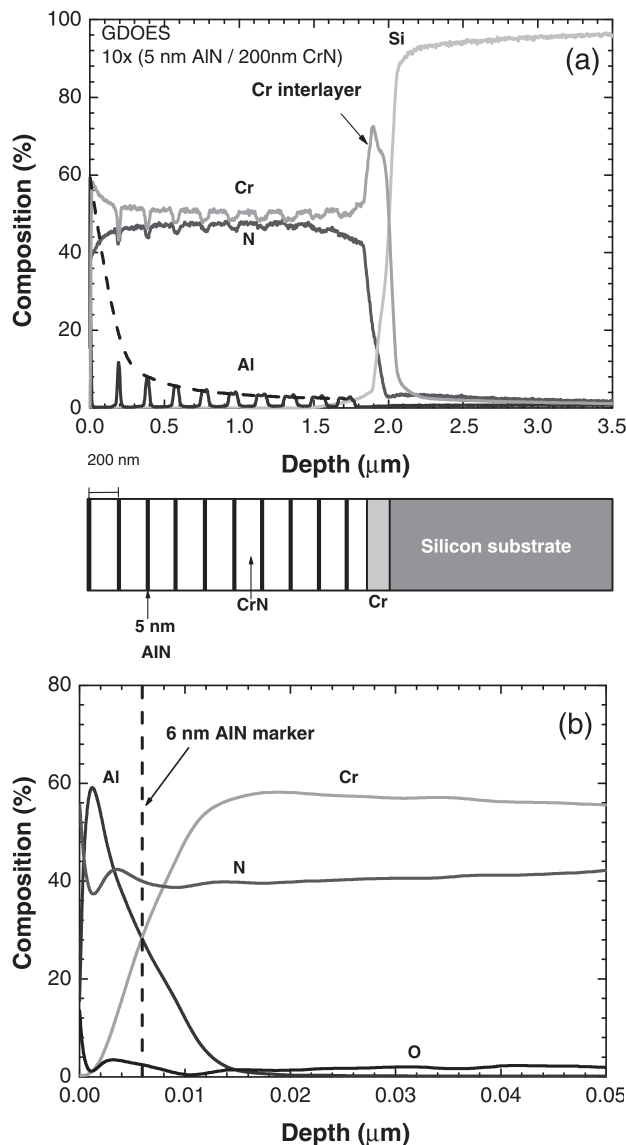

Fig. 8. GDOES depth profile of (a) multilayer 10× (5 nm AlN/200 nm AlN)/100 nm Cr. The dashed line shows the decrease of Al content in the AlN markers. In (b) the first 50 nm of the profile are shown. The vertical dashed line indicates the thickness of the first AlN ultrathin layer to be of 6 nm.

CrN/AlN interfaces (up to approximately 50 nm) increases linearly with depth and follows the trend observed for the thicker layers (degrading 40 nm/μm). After that, there is a clear decrease in the depth resolution, saturating at a value of 4–5 nm. A similar behaviour is observed for the AlN/CrN interfaces, although the initial increase is much less evident.

The depth resolution results for the different nitride multilayer systems studied (see Fig. 7) can be summarised as follows: (i) The depth resolution worsens linearly with the sputtering depth when there is no mixing of layers of the same material. This is the case for the thick trilayer system in the range of depths that we have studied, and for the first 400 nm of the bilayer system of alternating 35 nm CrN and 100 nm AlN. (ii) The layer mixing can be detected by a slope change in the depth resolution with depth. (iii) There is a saturation value for the depth resolution curve tending to be of half of the thickness of the thinner layer in the stack system (i.e. approximately 20 nm for the thin bilayer system and 5 nm for the ultrathin system). (iv) Although the layer mixing degrades substantially the composition profiles, the periodicity of the multilayer coatings is preserved in GDOES analysis even for ultrathin layers (<10 nm). (v) Extrapolating the depth resolution results to the beginning of the analysis (zero depth), an ultimate value of Δz=4–6 nm at the surface can be estimated.

In order to confirm this last result we have tested the system of 5 nm AlN layers embedded at increasing depths in a CrN matrix. Fig. 8(a) shows the depth profile of the GDOES analysis together with a scheme of the system studied (bottom panel). The ten AlN markers are perfectly detected although buried deep in the matrix. There is a fast degradation of the Al profile, but the first AlN layer at the outmost surface is perfectly resolved both in composition (55%) and in thickness (6 nm) as seen in Fig. 8(b). This matches with the calculation of the depth resolution using the "inverse maximum slope" method. Such method leads to a depth resolution of 5.8 nm at the surface and a linear increase of 40 nm/μm for the first three markers of the coating. These results coincide very precisely with the ones obtained for the previous studied multilayer nitride systems and give an extra proof of the ultimate depth resolution of our GDOES system.

4. Conclusions

This work shows the complementary capability of GDOES and RBS to study metal and metal nitride multilayer stacks currently used in technological applications, being able to resolve layer thickness ranging from hundreds of nanometers up to a few nanometers (superlattices). This has been demonstrated for the particular case of CrN/AlN multilayers, where the layered structure of the coatings have been verified by SEM and RBS analysis in order to discriminate and identify profile artefacts in the GDOES profile. The artefacts found when depth profiling by GDOES are related to the sputtering process in the glow discharge (surface roughening and crater geometry) and result in a worsening of the depth resolution by GDOES. The GDOES interfaces for above nitride coatings were found to be sharper than for similar metal systems (Ti/Cr), attributed to a lower sputtering rate. We have also observed that the depth resolution degrades linearly with depth with a rate of approximately 40 nm/μm. The mixing of consecutive layers can be detected by change of the slope of the depth resolution with depth. Actually, the depth resolution tends to saturate in a value close to half of the thinner component of the bilayer system. Extrapolating the depth resolution results of the different nitride systems studied to zero thickness (i.e. the surface) leads to a value of 4–6 nm. This result was confirmed by the accurate resolution, both in thickness and composition, of a 5-nm ultrathin AlN surface layer.

References

[1] S. Veprek, M.G.J. Veprek-Heijman, P. Karvankova, J. Prochazka, Different approaches to superhard coatings and nanocomposites, Thin Solid Films 476 (2005) 1–29.

[2] S. Zhang, D. Sun, Y. Fu, H. Du, Toughening of hard nanostructural thin films: a critical review, Surf. Coat. Technol. 198 (2005) 2–8.
[3] A. Leyland, A. Matthews, Design criteria for wear-resistant nanostructured and glassy-metal, Surf. Coat. Technol. 177–178 (2004) 317–324.
[4] J. Musil, Hard and superhard nanocomposite coatings, Surf. Coat. Technol. 125 (2000) 322–330.
[5] R. Payling, D. Jones, A. Bengtson (Eds.), Glow Discharge Optical Emission Spectrometry, John Wiley & Sons, 1997.
[6] M.R. Winchester, R. Payling, Radio-frequency glow discharge spectrometry: a critical review, Spectrochim. Acta Part B 59 (2004) 607–666.
[7] W.B. Teo, K. Hirokawa, Depth analysis of electrodeposited iron-nickel and copper-zinc alloy coatings by glow-discharge emission-spectroscopy, Surf. Interface Anal. 11 (1988) 533–538.
[8] W.B. Teo, K. Hirokawa, Depth analysis of metal coatings by glow discharge spectrometry with an argon helium gas mixture, Surf. Interface Anal. 14 (1989) 143–152.
[9] Z. Weiss, Depth analysis of nickel thin films on silicon by glow discharge spectroscopy: the interface region, Surf. Interface Anal. 15 (1990) 775–780.
[10] Z. Weiss, Quantitative-evaluation of depth profiles analyzed by glow discharge optical emission spectroscopy: analysis of diffusion processes, Spectrochim. Acta Part B 47 (1992) 859–876.
[11] S. Oswald, S. Baunack, Comparison of depth profiling techniques using ion sputtering from the practical point of view, Thin Solid Films 425 (2003) 9–19.
[12] F. Präßler, V. Hoffmann, J. Schumann, K. Wetzig, Comparison of depth resolution for direct current and radiofrequency modes in glow discharge optical emission spectrometry, J. Anal. At. Spectrom. 10 (1995) 677–680.
[13] V. Hodoroaba, W.E.S. Unger, H. Jenett, V. Hoffmann, B. Hagenhoff, S. Kayser, K. Wetzig, Depth profiling of electrically non-conductive layered samples by RF-GDOES and HFM plasma SNMS, Appl. Surf. Sci. 179 (2001) 30–38.
[14] R. Escobar Galindo, E. Forniés, J.M. Albella, Interfacial effects during the analysis of multilayer metal coatings by radio-frequency glow discharge optical emission spectroscopy: Part 1. Crater shape and sputtering rate effects, J. Anal. At. Spectrom. 20 (2005) 1108–1115.
[15] R. Escobar Galindo, E. Forniés, J.M. Albella, Interfacial effects during the analysis of multilayer metal coatings by radio-frequency glow discharge optical emission spectroscopy: Part 2. Evaluation of depth resolution function and application to thin multilayer coatings, J. Anal. At. Spectrom. 20 (2005) 1116–1120.
[16] V. Hoffmann, R. Dorka, L. Wilken, V.D. Hodoroaba, K. Wetzig, Present possibilities of thin-layer analysis by GDOES, Surf. Interface Anal. 35 (7) (2003) 575–582.
[17] A. Quentmeier, in: R. Payling, D.G. Jones, A. Bengston (Eds.), Glow Discharge Optical Emission Spectroscopy, John Wiley & Sons, 1997, Section 7.1 and Section 7.2.
[18] J. Angeli, A. Bengston, A. Bogaerts, V. Hoffmann, V. Hodoroaba, E. Steers, Glow discharge optical emission spectrometry: moving towards reliable thin film analysis: a short review, J. Anal. At. Spectrom. 18 (2003) 670–679.
[19] A. Thobor, C. Rousselot, S. Mikhailov, Depth profiles study of n(TiN/AlN) bilayers systems by GDOES and RBS techniques, Surf. Coat. Technol. 174–175 (2003) 351–359.
[20] A. Quentmeier, in: R. Payling, D.G. Jones, A. Bengston (Eds.), Glow Discharge Optical Emission Spectroscopy, John Wiley & Sons, 1997, Section 7.3.
[21] Z. Weiss, in: R. Payling, D.G. Jones, A. Bengston (Eds.), Glow Discharge Optical Emission Spectroscopy, John Wiley & Sons, 1997, Section 7.5.
[22] U. Beck, G. Reiners, Th. Wirth, V. Hoffmann, F. Präßler, Multilayer reference coatings for depth profile standards, Thin Solid Films 290–291 (1996) 57–62.
[23] K. Shimizu, G.M. Brown, H. Habazaki, K. Kobayashi, P. Skeldon, G.E. Thompson, G.C. Wood, Glow discharge optical emission spectrometry (GDOES) depth profiling analysis of anodic alumina films: a depth resolution study, Surf. Interface Anal. 27 (1999) 24–28.
[24] K. Shimizu, G.M. Brown, H. Habazaki, K. Kobayashi, P. Skeldon, G.E. Thompson, G.C. Wood, Impurity distributions in barrier anodic films on aluminium: a GDOES depth profiling study, Electrochim. Acta 44 (1999) 2297–2306.
[25] K. Shimizu, H. Habazaki, P. Skeldon, G.E. Thompson, Impact of RF-GD-OES in practical surface analysis, Spectrochim. Acta Part B 58 (2003) 1573–1583.
[26] K. Shimizu, H. Habazaki, P. Skeldon, G.E. Thompson, Radiofrequency GDOES: a powerful technique for depth profiling analysis of thin films, Surf. Interface Anal. 35 (2003) 564–574.
[27] K. Shimizu, H. Habazaki, P. Skeldon, G.E. Thompson, R.K. Marcus, Influence of interfacial depth on depth resolution during GDOES depth profiling analysis of thin alumina films, Surf. Interface Anal. 31 (2001) 869–873.
[28] S. Oswald, V. Hoffmann, G. Ehrlich, Contributions to computer-aided interpretation of ion sputtering depth profiling, Spectrochim. Acta Part B 49 (1994) 1123–1145.
[29] M.A. Auger, R. Gago, M. Fernández, O. Sánchez, J.M. Albella, Deposition of TiN/Al bilayers on a rotating substrate by reactive sputtering, Surf. Coat. Technol. 157 (2002) 26–33.
[30] A. Climent-Font, F. Pászti, G. García, M.T. Fernández-Jiménez, F. Agulló, First measurements with the Madrid 5 MV tandem accelerator, Nucl. Instrum. Methods Phys. Res., B 219–220 (2004) 400–404.
[31] D.F. Herring, R. Chiba, B.R. Gasten, H.T. Richards, N-14(α,α)N-14 and N-14(α,p)O-17 differential cross sections, Phys. Rev. 112 (1958) 1210–1216.
[32] M. Mayer, SIMNRA User's Guide, IPP report 9/113, Max Plank Institute (1997).
[33] http://www.jobinyvon.com.
[34] E. Forniés, R. Escobar Galindo, O. Sánchez, J.M. Albella, Growth and characterization of CrN_x deposited by DC reactive magnetron sputtering, Surf. Coat. Technol. 200 (2006) 6047–6053.
[35] V. Hoffmann, R. Kurt, K. Kammer, R. Thielsch, Th. Wirth, U. Beck, Interference phenomena at transparent layers in glow discharge optical emission spectrometry, Appl. Spectrosc. 53 (1999) 987–990.
[36] R. Dorka, R. Kunze, V. Hoffmann, Investigation of SiO2 layers by glow discharge optical emission spectroscopy including layer thickness determination by an optical interference effect, J. Anal. At. Spectrom. 15 (2000) 873–876.
[37] http://ece-www.colorado.edu/~bart/book/ellipstb.htm.
[38] S. Hofmann, in: D. Briggs, M.P. Seah (Eds.), Practical Surface Analysis by Auger and X-ray Photoelectron Spectroscopy, John Wiley & Sons, 1983, Chap. 4.
[39] S. Hofmann, From depth resolution to depth resolution function: refinement of the concept for delta layers, single layers and multilayers, Surf. Interface Anal. 27 (1999) 825–834.
[40] J. Pisonero, B. Fernández, R. Pereiro, N. Bordel, A. Sanz-Medel, Glow-discharge spectrometry for direct analysis of thin and ultra-thin solid films, TrAC, Trends Anal. Chem. 25 (2006) 11–18.
[41] V. Hoffmann, M. Kasik, P.K. Robinson, C. Venzago, Glow discharge mass spectrometry, Anal. Bioanal. Chem. 381 (2005) 173–188.
[42] R. Escobar Galindo, E. Forniés, J.M. Albella, Compositional depth profiling analysis of thin and ultrathin multilayer coatings by radio-frequency glow discharge optical emission spectroscopy, corrected proof in Surf. Coat. Technol (in press).